02,01,07

On the abrupt change in the superconducting order parameter in the vicinity of the $s_{\pm} \rightarrow s_{++}$ transition in the Born limit

© V.A. Shestakov, M.M. Korshunov

Kirensky Institute of Physics, Federal Research Center KSC SB, Russian Academy of Sciences, Krasnoyarsk, Russia

E-mail: v_shestakov@iph.krasn.ru

Received March 6, 2025
Revised March 6, 2025
Accepted May 5, 2025

In multiband systems like iron pnictides and chalcogenides, the unconventional superconducting state can emerge. Effect of disorder on this state may have unexpected consequences, such as, for instance, change of the $s_{\pm}$ superconducting order parameter structure to the s_{++} one. Studying of a system behavior near such a transition is very important. For this purpose, the grand thermodynamic potential for the normal, Ω_N, and superconducting, Ω_S, states is calculated, as well as their difference $\Delta\Omega = \Omega_S - \Omega_N$. An expression for $\Delta\Omega$ is derived for a two-band model of iron-based superconductors with the nonmagnetic impurities. The presence of disorder is considered within the T-matrix approximation for a multiband Eliashberg theory. Near the Born limit in the vicinity of $s_{\pm} \rightarrow s_{++}$ transition, two sets of solutions, which are obtained for opposite directions in changing of the impurity scattering rate, are found to exist. Based on $\Delta\Omega$, a phase diagram showing energetically favorable solutions for $s_{\pm}$ and s_{++} states as well as the transition between them is plotted. At low temperatures within the region where two sets of solutions coexist, the transition is abrupt and barely dependent on temperature. At higher temperatures, the Eliashberg equations have a single set of solutions, with the transition between $s_{\pm}$ and s_{++} states being smooth.

Keywords: unconventional superconductivity, iron pnictides, iron chalcogenides, grand thermodynamic potential, impurity scattering, Eliashberg equations.

DOI: 10.61011/PSS.2025.07.61880.35HH-25

1. Introduction

The discovery of superconductivity in iron pnictides stimulated the development of interest in multiband systems [1–5]. The ideas proposed decades ago for two-band superconductivity [6,7] have gained new life with the discovery of iron-based superconductors [8,9]. The order parameter with $s_{\pm}$ gap function changing its sign between different bands, was proposed as the dominant instability in the Cooper channel, which was confirmed in experiments on inelastic neutron scattering [10–12], quasiparticle interference [13], and Andreev reflection measurements [14].

A distinctive feature of iron-based superconductors, which distinguishes them from a large family of unconventional superconductors, is their robustness to superconductivity suppression by non-magnetic impurities [15–18]. This property is related to the possibility of changing the structure of the superconducting order parameter with the addition of non-magnetic impurities [19,20]. Such a change is a transition from a $s_{\pm}$-state with a gap function that changes its sign between bands to a state with a sign-preserving gap function of the s_{++}-type.

Experimentally, such a transition can be detected by changing the London penetration depth for a superconductor with a nonmagnetic disorder [21]. There are at least two independent reports on the experimental observation of this transition [22,23].

The transition is significantly influenced by the strength of the impurity potential [24,25], namely: for a weak scattering potential, in the so-called Born limit, the transition (a change in the sign of a gap in one of the bands) is characterized by a sharp change in the order parameter, while for a larger impurity potential this change is smooth and accompanied with gradual passing of one of the gaps through zero. The multiband analogue of Anderson's theorem holds in the unitary limit of the strong scattering potential of an impurity [6,26], and there is no transition. The nature of the abrupt transition near the Born limit is still unclear. There are a number of studies [27–30], in which it is assumed that this transition can pass through a state with broken time-reversal symmetry and that this state has been observed experimentally [31]. We showed in Ref. [32] that such a state is not realized in the two-band model, unlike the study in Ref. [30]. Comparison with the results obtained in other studies is impossible without adding the third band [27–29,31] to the model used here, or without considering the external magnetic field induced by superconducting currents [29].

In order to shed light on the details of the transition $s_{\pm} \rightarrow s_{++}$ near the Born limit, in this paper we use the Grand thermodynamic potential (also called the Landau free energy) Ω, calculated for a two-band model to refine the phase diagram of the transition under consideration in the disorder-temperature axes.

2. Model

In this paper, we use a two-band model of iron-based superconductors with non-magnetic impurities [19,20] in terms of ξ-integrated Green functions $\widehat{\mathbf{g}}(i\omega_n)$ defined in a combined band space (matrices are denoted with bold-face font) and Nambu space (matrices are denoted with „$\widehat{\ }$“), and depending on the fermionic Matsubara frequency $i\omega_n$,

$$[\widehat{\mathbf{g}}(i\omega_n)]_{\alpha\beta} = \left[\int \widehat{\mathbf{G}}(\mathbf{k}, i\omega_n) d\xi(\mathbf{k})\right]_{\alpha\beta} = -\pi N_\alpha \frac{i\tilde{\omega}_{\alpha n}\widehat{\tau}_0 + \tilde{\phi}_{\alpha n}\widehat{\tau}_2}{\sqrt{\tilde{\omega}_{\alpha n}^2 + \tilde{\phi}_{\alpha n}^2}}\delta_{\alpha\beta}, \quad (1)$$

where N_α is the density of states at the Fermi level in the band with index $\alpha = (a, b)$ in the normal state, $i\tilde{\omega}_{\alpha n}$ and $\tilde{\phi}_{\alpha n}$ are the Matsubara frequency and the superconducting order parameter, respectively, renormalized by superconducting interaction and nonmagnetic impurity scattering, $\widehat{\tau}_j$ are Pauli matrices in Nambu space. The following system of units is adopted here: $\hbar = k_B = 1$. Thus, the temperature T and the frequency $\omega_n = (2n+1)\pi T$ are set in energy units. It should be noted that there are no terms proportional to the Pauli matrices $\widehat{\tau}_1$ and $\widehat{\tau}_3$. In the first case, the summand is omitted, taking into account the symmetry in the Nambu space of the equations on the order parameter [33], while in the second case, the summand vanishes due to the ξ-integration procedure.

The Matsubara frequencies and the order parameter are self-consistently renormalized by the self-energy as follows:

$$i\tilde{\omega}_{\alpha n} = i\omega_n - \Sigma_{0\alpha}^{\mathrm{SC}}(i\tilde{\omega}_{an}, i\tilde{\omega}_{bn}, \tilde{\phi}_{an}, \tilde{\phi}_{bn}) - \Sigma_{0\alpha}^{\mathrm{imp}}(i\tilde{\omega}_{an}, i\tilde{\omega}_{bn}, \tilde{\phi}_{an}, \tilde{\phi}_{bn}), \quad (2)$$

$$\tilde{\phi}_{\alpha n} = \Sigma_{2\alpha}^{\mathrm{SC}}(i\tilde{\omega}_{an}, i\tilde{\omega}_{bn}, \tilde{\phi}_{an}, \tilde{\phi}_{bn}) + \Sigma_{2\alpha}^{\mathrm{imp}}(i\tilde{\omega}_{an}, i\tilde{\omega}_{bn}, \tilde{\phi}_{an}, \tilde{\phi}_{bn}), \quad (3)$$

where the term $\Sigma_{0,2\alpha}^{\mathrm{SC}}$ in the self-energy is related to the pairing interaction and depends on the matrix 2×2 of coupling constants with elements in the band space. The matrix $\boldsymbol{\lambda}$ is an analog of the electron-phonon coupling constant, and, like the electron-phonon coupling constant, it determines the critical temperature. The pairing is determined by the spectral function $B(\Omega)$, reflecting the frequency dependence of spin fluctuations [19]. The term $\Sigma_{0,2\alpha}^{\mathrm{imp}}$ refers to scattering by non-magnetic impurities and is calculated within the T-matrix approximation, which is equivalent to the approximation of noncrossing diagrams. The indexes „0“ and „2“ point to the corresponding Pauli matrices $\widehat{\tau}_i$. The equations (2) and (3) represent the system of Eliashberg equations for a multiband superconductor with nonmagnetic impurities [19].

3. Landau free energy

In the most general form, the Grand thermodynamic potential or Landau free energy is given by the Luttinger–Ward expression for a multi-band system [34,35] with generalization to the case of a superconductor with nonmagnetic impurities:

$$\Omega_S(T) = -T\sum_{\omega_n \mathbf{k}} \mathrm{Tr}\left[\ln\left\{-\widehat{\mathbf{G}}^{-1}(\mathbf{k}, i\omega_n)\right\} + \widehat{\Sigma}(\mathbf{k}, i\omega_n)\widehat{\mathbf{G}}(\mathbf{k}, i\omega_n)\right] + \Omega'_{\mathrm{SC}}(T) + \Omega'_{\mathrm{imp}}(T), \quad (4)$$

$$\Omega'_{\mathrm{SC}}(T) = \frac{T}{2}\sum_{\mathbf{k},\omega_n} \mathrm{Tr}\left[\widehat{\Sigma}_{\mathrm{SC}}(\mathbf{k}, i\omega_n)\widehat{\mathbf{G}}(\mathbf{k}, i\omega_n)\right], \quad (5)$$

$$\Omega'_{\mathrm{imp}}(T) = n_{\mathrm{imp}} T\sum_{\omega_n,\mathbf{k}} \mathrm{Tr}\left[\sum_{t=1}^{\infty}\frac{1}{t}\left(\widehat{\mathbf{U}}\widehat{\mathbf{G}}(\mathbf{k}, i\omega_n)\right)^t\right], \quad (6)$$

where the Green's function $\widehat{\mathbf{G}}$ and the self-energy $\widehat{\Sigma}$ are written in general form and depend on both the momentum $\mathbf{k}$ and the Matsubara frequency ω_n, with the sum over momenta, $\sum_{\mathbf{k}}$ denoting integration over the entire first Brillouin zone, $\sum_{\mathbf{k}} \leftrightarrow \int_{\mathrm{IBZ}} \mathrm{d}^3k/(2\pi)^3$, leading to the expression (1) for the Green's function and for the self-energy, included in the equations (2) and (3). The explicit form of latter is given in Ref. [19]. The matrix of the scattering potential of impurities $\widehat{\mathbf{U}}$ has the following form:

$$\left\{\widehat{\mathbf{U}}\right\}_{\alpha\beta} = [u + (v-u)\delta_{\alpha\beta}] \otimes \widehat{\tau}_3, \quad (7)$$

where v and u are the intraband and interband components of the impurity potential, respectively, trace $\mathrm{Tr}[\ldots]$ is taken over all subspaces (Nambu space and band indexes). In equations (4)–(6), the values $\Omega'_{\mathrm{SC}}(T)$ and $\Omega'_{\mathrm{imp}}(T)$ denote parts of the Luttinger–Ward functional related to superconducting pairing and scattering on impurities, respectively, calculated within the same diagrammatic approximation as the corresponding terms of the self-energy used in calculating $i\tilde{\omega}_{\omega n}$ and $\tilde{\phi}_{\alpha n}$ in equations (2) and (3). Despite the designation, the term $\Omega'_{\mathrm{SC}}(T)$ is not exclusively related to the superconducting state, since the effective interaction between particles is also present in the normal state, renormalizing the Matsubara frequencies.

In practice, it is more convenient to consider the difference between free energies in the superconducting and normal state:

$$\Delta\Omega(T) = \Omega_{\mathrm{S}}(T) - \Omega_{\mathrm{N}}(T), \quad (8)$$

where the expression for the Landau free energy of the system in the normal state Ω_{N} has a form similar to the expression (4), with the only difference that all values are calculated under the condition $\tilde{\phi}_{\alpha n} = 0$. Within the

framework of the two-band model considered in this paper, this difference has the following form:

$$\Delta\Omega(T) = -\pi T \sum_{\omega_n} \sum_{\alpha=a,b} N_\alpha \left[\frac{\omega_n \tilde{\omega}_{\alpha n}}{\sqrt{\tilde{\omega}_{\alpha n}^2 + \tilde{\phi}_{\alpha n}^2}} + \sqrt{\tilde{\omega}_{\alpha n}^2 + \tilde{\phi}_{\alpha n}^2} - |\omega_n| - |\tilde{\omega}_{\alpha n}^{\mathrm{N}}| \right] + \Delta\tilde{\Omega}(T), \quad (9)$$

where $\tilde{\omega}_{\alpha n}^N$ are the Matsubara frequencies renormalized by superconducting interaction and impurity scattering in the normal state,

$$\Delta\tilde{\Omega}(T) = \pi T N_a \Gamma_a \sum_{\omega_n} \left[\frac{2\sigma(1-\eta^2)^2 + (1-\sigma)\kappa}{2D} - \frac{2\sigma(1-\eta^2)^2 + (1-\sigma)\kappa^{\mathrm{N}}}{2D^{\mathrm{N}}} \right] - n_{\mathrm{imp}} T \sum_{\omega_n} \ln(D/D^{\mathrm{N}}), \quad (10)$$

$$\kappa = \eta^2 \frac{N_a^2 + N_b^2}{N_a N_b} + 2 \frac{\tilde{\omega}_{an}\tilde{\omega}_{bn} + \tilde{\phi}_{an}\tilde{\phi}_{bn}}{\sqrt{\tilde{\omega}_{an}^2 + \tilde{\phi}_{an}^2}\sqrt{\tilde{\omega}_{bn}^2 + \tilde{\phi}_{bn}^2}}, \quad (11)$$

$$D = (1-\sigma)^2 + \sigma^2(1-\eta^2)^2 + \sigma(1-\sigma)\kappa, \quad (12)$$

$$\kappa^{\mathrm{N}} = \kappa\big|_{\tilde{\phi}_{an}=0}, \quad D^{\mathrm{N}} = D\big|_{\tilde{\phi}_{an}=0},$$

$\eta = v/u$ is the ratio of the intraband component of the impurity potential to the interband component, σ is the effective cross section:

$$\sigma = \frac{\pi^2 N_a N_b u^2}{1 + \pi^2 N_a N_b u^2}, \quad (13)$$

n_{imp} is the impurity concentration, and Γ_a is the impurity scattering rate,

$$\Gamma_a = \frac{2 n_{\mathrm{imp}} \sigma}{\pi N_a} = 2 N_{\mathrm{imp}} \pi N_b u^2 (1-\sigma), \quad (14)$$

setting the presence of non-magnetic disorder in the system. The effective cross-section shows the strength of the scattering potential of impurities and varies from zero for weak impurity scattering in the Born limit ($\pi u N_\alpha \ll 1$) to unity in the unitary limit of strong scattering impurities ($\pi u N_\alpha \gg 1$). In the Born limit, $\sigma \to 0$, the contribution of $\Delta\tilde{\Omega}$ in the expression (9) is cancelled and $\Delta\Omega$ depends on impurities implicitly through a self-consistent solution of the equations (2) and (3).

4. Results and discussion

In the calculations below, we use the following values for the elements of the matrix of coupling constants $\{\lambda_{aa}, \lambda_{ab}, \lambda_{ba}, \lambda_{bb}\} = \{3.0, -0.2, -0.1, 0.5\}$. This combination leads to a superconducting state below the critical temperature in the pure limit $T_{c0} = 40\,\mathrm{K}$ with a $s_\pm$-order parameter and a positive band-averaged coupling constant $\langle\lambda\rangle = (N_a[\lambda_{aa} + \lambda_{ab}] + N_b[\lambda_{ba} + \lambda_{bb}])/(N_a + N_b)$. It is the superconducting state with such an order parameter structure in which non-magnetic impurities cause the transition $s_\pm \to s_{++}$. Here we assume that impurity scattering occurs only in the interband channel ($\eta = 0$), since, as shown earlier, a nonzero value of the intraband component of the impurity scattering potential does not affect the superconducting state in the Born limit and only shifts the transition point to higher values of Γ_a at $\sigma \neq 0$ [24]. The density of states in each of the bands is set such that ($N_a = 1.0656\,\mathrm{eV}^{-1}$ per unit cell and $N_b = 2N_a$) the total density of states is $N = N_a + N_b$ being close to the values obtained within the first-principle calculations [36,37].

4.1. Hysteresis of solutions to the Eliashberg equations

It was previously shown that the transition between $s_\pm$- and s_{++}-states for the effective cross section $\sigma < 0.12$ and temperatures $0.03 < T < 0.1T_{c0}$ occurs abrupt, i.e., the order parameter within one of the bands sharply changes its sign [24]. Here we show that the Eliashberg equations (2) and (3) have two types of solutions within the range of values $0 < \sigma < 0.18$ and temperatures $0.03 < T < 0.1T_{c0}$. They are obtained when moving in opposite directions along the axis Γ_a. In other words, to obtain the first type of solutions, we solve the Eliashberg equations in the pure limit, $\Gamma_a = 0$. Next, we add impurities, and the results of the solution obtained in the pure limit are used as seed values. In the following steps, we repeat the procedure: increase Γ_a and use the solutions from the previous step as seed values. Thus, we construct the evolution of a superconductor from pure to being in a „impure/disordered“ state. The second set of solutions is obtained by reversing the direction of the system's evolution, i.e., we start with the „dirty“ limit ($\Gamma_a = 6T_{c0}$) in calculations, and then reduce the disorder in the system down to the clean limit by reducing Γ_a and using solutions for large Γ_a as seed values for calculating solutions at lower impurity scattering rates. These two types of solutions are shown in Figure 1, where the function of the superconducting gap

$$\Delta_{b,n} = \omega_n \tilde{\phi}_{b,n}/\tilde{\omega}_{b,n}, \quad (15)$$

in the band b for the first Matsubara frequency ($n = 0$) is represented for the Born limit for different temperatures $0.01 < T < 0.10T_{c0}$ depending on Γ_a. The superconducting gap function determines the superconducting order parameter and corresponds to a gap in the spectrum of electronic excitations in the band b. The behavior of the function $\Delta_{b,n>0}$ corresponds to the behavior of $\Delta_{b,0}$, so further in the discussion we can omit the subscript „0“, talking about the behavior of the gap function in the band b as a whole. We observe the effect of hysteresis between solutions for a system evolving from a clean state to a „dirty“ one (denoted by lines with hollow symbols and the word „forward“) and in the opposite direction (denoted by shaded

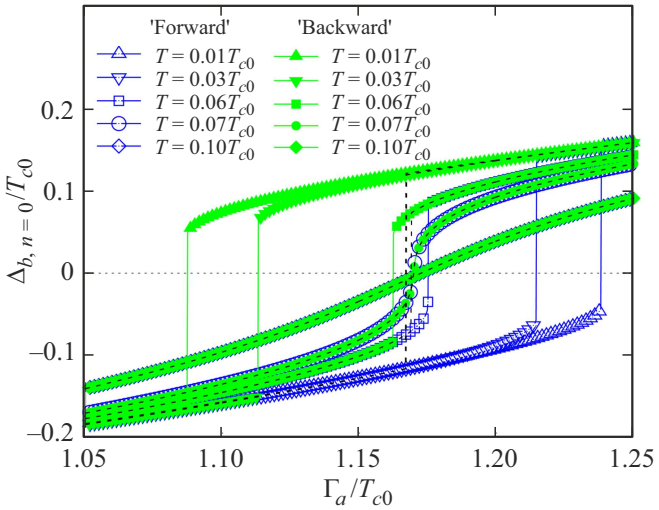

Figure 1. Graphs of the dependence of the superconducting gap on Γ_a in the Born limit for the first Matsubara frequency, $n = 0$, in the band b for various temperatures. The designation „forward“ indicates the evolution of the system from a pure limit to a disordered state „backward“ indicates the reverse direction of the evolution of the system. The black dotted lines show solutions corresponding to the lowest free Landau energy. Hereafter, the values of the gap function $\Delta_{b,0}$, the intensity of scattering by impurities Γ_a and temperature T are given in units of the critical temperature for a pure superconductor T_{c0}.

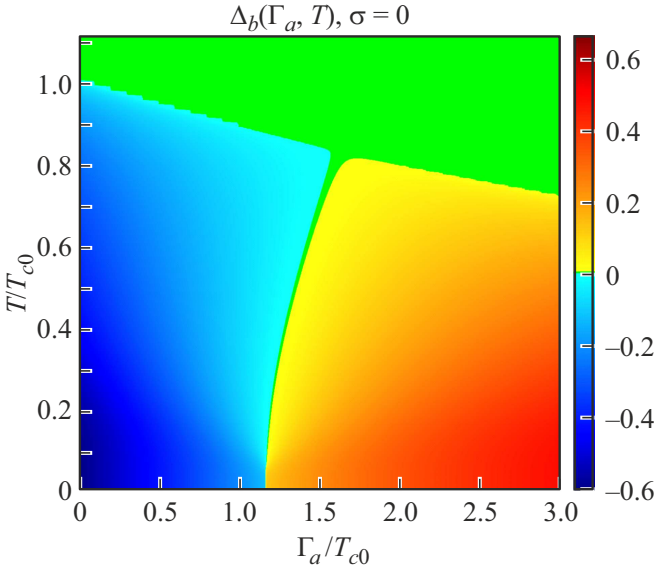

Figure 2. Phase diagram for the superconducting slit $\Delta_{b,0}$ in the band b for the first Matsubara frequency, $n = 0$, in the axes (Γ_a, T). The colors correspond to the sign and amplitude of $\Delta_{b,0}$: red — positive, blue — negative, green — zero values.

symbols and the word „backward“). As the temperature increases, the width of the hysteresis loop decreases until it collapses at $T \approx 0.07T_{c0}$, when the solutions for both directions („forward“ and „backward“) begin to coincide for all values of Γ_a.

4.2. Phase diagram

In order to resolve the question of how to choose a single set of solutions from two competing ones, the natural approach is to choose the most energy-favourable solutions. Comparing the Landau free energy differences $\Delta\Omega$ calculated using the equation (6), we select solutions with the lowest value $\Delta\Omega$ and construct a phase diagram for the superconducting gap $\Delta_{b,0}$, shown in Figure 2.

The phase diagram is plotted in axes (Γ_a, T). The intensity of scattering on impurities varies within $0 < \Gamma_a < 2.5T_{c0}$, the temperature: $0.01 < T < 1.1T_{c0}$. The sign and amplitude of the gap function, which determine whether the system is in $s_{\pm}$-, s_{++}-, or the normal state, are indicated by color gradations: blue indicates the negative sign (opposite to the sign of the second gap $\Delta_{a,0}$, i. e. $s_{\pm}$-state), red indicates the positive sign (corresponding to the sign $\Delta_{a,0}$, i. e. s_{++}-state), green indicates values close to zero $\Delta_{b,0}$. Since below T_c the gap in the second band $(\Delta_{a,0})$ does not vanish, the zero values of the gap $\Delta_{b,0}(T < T_c)$ correspond to the so-called „gapless“ superconducting, but not the normal state. That is, the superconducting gap in the spectrum of single-electron excitations is closed only within the band b, while it remains finite within the band a. An almost vertical line is observed separating the $s_{\pm}$- and s_{++}-states from each other in the phase diagram at low temperatures $(T < 0.07T_{c0})$ and values Γ_a close to $1.16T_{c0}$, which results in a sudden color change from blue to red without a smooth transition. Here $\Delta_{b,0}$ changes its sign abruptly. At temperatures $T > 0.07T_{c0}$, the transition $s_{\pm} \rightarrow s_{++}$ is smooth and strong temperature-dependent (at such temperatures, the line $\Delta_{b,0} = 0$ has a more pronounced slope than in the jump transition region).

We previously obtained a similar result only for the „forward“ evolution of the system with a change in the contribution of the non-magnetic disorder [25]. The main difference is that the line of abrupt sign change Δ_b at low temperatures $T < 0.1T_{c0}$ strongly depends on temperature, i. e. it has a more pronounced slope due to the presence of energy-unfavourable solutions. In this paper, we avoid this by comparing the free energies and choosing a set with a lower value, thereby refining the form of the phase diagram.

5. Conclusion

For a multi-band superconductor with non-magnetic impurities in the region of a sharp transition between $s_{\pm}$- and s_{++}-states, the Eliashberg equations may have more than one set of solutions near the Born limit ($\sigma < 0.18$). Two different sets of solutions are obtained for opposite directions of the system's evolution relative to changes in the intensity of scattering by impurities. Such a hysteresis exists in a limited range of temperatures and the impurity scattering rates. In order to eliminate ambiguity in choosing a solution, we calculated the Landau free energy difference $\Delta\Omega = \Omega_S - \Omega_N$ and, choosing solutions with the lowest value of $\Delta\Omega$, we constructed the phase diagram displaying

$s_{\pm}$- and s_{++}-states and the transition between them. The phase diagram shows an almost straight line of sharp transition $s_{\pm} \rightarrow s_{++}$, directed along the temperature axis, starting from $T_{\min} = 0.01T_{c0}$ and ending at $T \approx 0.07T_{c0}$. A sharp transition is characterized by a jump in the gap Δ_b when its sign changes. At temperatures above $T \approx 0.07T_{c0}$, the abrupt feature of the transition between $s_{\pm}$- and s_{++}-states is interchanged to a smooth one, in which the gap Δ_b changes continuously with a change in the impurity scattering rate. Our result refines the phase diagram [25], which was obtained only for an increasing amount of disorder in the system and temperatures limited from below by the value $T = 0.03T_{c0}$.

Funding

The study was carried within the state assignment of Kirensky Institute of Physics.

Conflict of interest

The authors declare that they have no conflict of interest.

References

[1] M.B. Sadovsky. UFN **178**, 1243–1271 (2008). (in Russian).
[2] Yu.A. Izyumov, E.Z. Kurmaev. UFN **178**, 1307–1334 (2008). (in Russian).
[3] A.L. Ivanovsky. UFN **178**, 1273–1306 (2008). (in Russian).
[4] G.R. Stewart. Rev. Mod. Phys. **83**, *4*, 1589–1652 (2011).
[5] P.J. Hirschfeld, M.M. Korshunov, I.I. Mazin Rep. Prog. Phys. **74**, 124508 (2011).
[6] A. Golubov, I. Mazin. Physica C: Supercond. **243**, 153–159 (1995).
[7] A.A. Golubov, I.I. Mazin. Phys. Rev. B **55**, *22*, 15146–15152 (1997).
[8] I.I. Mazin, D.J. Singh, M.D. Johannes, M.H. Du. Phys. Rev. Lett. **101**, *5*, 057003 (2008).
[9] D. Parker, O.V. Dolgov, M.M. Korshunov, A.A. Golubov, I.I. Mazin. Phys. Rev. B **78**, *13*, 134524 (2008).
[10] M.D. Lumsden, A.D. Christianson. J. Phys. Condens. Matter, **22**, 203203 (2010).
[11] D. Inosov. C.R. Physique **17**, 60–89 (2016).
[12] M.M. Korshunov. Phys. Rev. B **98**, *10*, 104510 (2018).
[13] J.E. Hoffman. Rep. Prog. Phys. **74**, 124513 (2011).
[14] M.M. Korshunov, S.A. Kuzmichev, T.E. Kuzmicheva. Materials **15**, 6120 (2022).
[15] A.E. Karkin, J. Werner, G. Behr, B.N. Goshchitskii. Phys. Rev. B **80**, *17*, 174512 (2009).
[16] A.E. Kar'kin, T. Wolf, A.N. Wasil'ev, O.S. Volkova, B.N. Goshchitskii. Phys. Metals. Metallogr. **113**, 455 (2012).
[17] K. Cho, M. Kończykowski, J. Murphy, H. Kim, M.A. Tanatar, W.E. Straszheim, B. Shen, H.H. Wen, R. Prozorov. Phys. Rev. B **90**, *10*, 104514 (2014).
[18] R. Prozorov, M. Kończykowski, M.A. Tanatar, A. Thaler, S.L. Bud'ko, P.C. Canfield, V. Mishra, P.J. Hirschfeld. Phys. Rev. X **4**, *4*, 041032 (2014).
[19] M.M. Korshunov, Yu.N. Togushova, O.V. Dolgov. UFN **186**, 1315–1347 (2016). (in Russian).
[20] D.V. Efremov, M.M. Korshunov, O.V. Dolgov, A.A. Golubov, P.J. Hirschfeld. Phys. Rev. B **84**, *18*, 180512 (2011).
[21] V.A. Shestakov, M.M. Korshunov., Y.N. Togushova, O.V. Dolgov. Supercond. Sci. Technol. **34**, 075008 (2021).
[22] M.B. Schilling, A. Baumgartner, B. Gorshunov, E.S. Zhukova, V.A. Dravin, K.V. Mitsen, D.V. Efremov, O.V. Dolgov, K. Iida, M. Dressel, S. Zapf. Phys. Rev. B **93**, *17*, 174515 (2016).
[23] G. Ghigo, D. Torsello, G.A. Ummarino, L. Gozzelino, M.A. Tanatar, R. Prozorov, P.C. Canfield. Phys. Rev. Lett. **121**, *10*, 107001 (2018).
[24] V.A. Shestakov, M.M. Korshunov, Y.N. Togushova, D.V. Efremov, O.V. Dolgov. Supercond. Sci. Technol. **31**, 034001 (2018.)
[25] V.A. Shestakov, M.M. Korshunov, O.V. Dolgov. Symmetry **10**, 323 (2018).
[26] P.W. Anderson. J. Phys. Chem. Solids **11**, 26 (1959).
[27] V. Stanev. Supercond. Sci. Technol. **28**, *1*, 014006 (2014).
[28] J. Garaud, M. Silaev, E. Babaev. Physica C: Supercond. **533**, 63 (2017).
[29] J. Garaud, A. Corticelli, M. Silaev, E. Babaev. Phys. Rev. B **97**, *5*, 054520 (2018).
[30] M. Silaev, J. Garaud, E. Babaev. Phys. Rev. B **95**, *2*, 024517 (2017).
[31] V. Grinenko, R. Sarkar, K. Kihou, C.H. Lee, I. Morozov, S. Aswartham, B. Büchner, P. Chekhonin, W. Skrotzki, K. Nenkov, R. Hühne, K. Nielsch, S.-L. Drechsler, V.L. Vadimov, M.A. Silaev, P.A. Volkov, I. Eremin, H. Luetkens, H.-H. Klauss. Nat. Phys. **16**, *7*, 786 (2020).
[32] V.A. Shestakov, M.M. Korshunov. Supercond. Sci. Technol. **38**, *5*, 055002 (2025).
[33] V.A. Shestakov, M.M. Korshunov. FTT **66**, *8*, 1258 (2024). (in Russian).
[34] J.M. Luttinger, J.C. Ward. Phys. Rev. **118**, *5*, 1417–1427 (1960).
[35] J.M. Luttinger. Phys. Rev. **119**, *4*, 1153–1163 (1960).
[36] J. Ferber, Y.Z. Zhang, H.O. Jeschke, R. Valentí. Phys. Rev. B **82**, *16*, 165102 (2010).
[37] M.V. Sadovskii, E.Z. Kuchinskii, I.A. Nekrasov. J. Magn. Magn. Mater. **324**, 3481 (2012).

Translated by A.Akhtyamov